Evaluation of Corroded OPS Fibre-Concrete using NDT Method

Ahmad Zaki[1,2]*, Sri Atmaja P. Rosyidi[1], Ni Nyoman Kencanawati[3], Syarizal Fonna[4], Zainah Ibrahim[5], Hammad R. Khalid[6,7], Mohammed A. Al-Osta[6,7]

[1] Department of Civil Engineering
   Universitas Muhammadiyah Yogyakarta, Bantul, Yogyakarta, 55183, INDONESIA

[2] Magister of Civil Engineering
   Universitas Muhammadiyah Yogyakarta, Bantul, Yogyakarta, 55183, INDONESIA

[3] Department of Civil Engineering
   Universitas Mataram, Mataram, Nusa Tenggara Barat, 83115, INDONESIA

[4] Department of Mechanical and Industrial Engineering
   Universitas Syiah Kuala, Banda Aceh, Nanggroe Aceh Darussalam, 23111, INDONESIA

[5] Department of Civil Engineering
   University of Malaya, Wilayah Persekutuan Kuala Lumpur, 50603, MALAYSIA

[6] Department of Civil and Environmental Engineering
   King Fahd University of Petroleum and Minerals, Dhahran, 31261, KINGDOM OF SAUDI ARABIA

[7] Interdisciplinary Research Centre for Construction and Building Materials
   King Fahd University of Petroleum and Minerals, Dhahran, 31261, KINGDOM OF SAUDI ARABIA

*Corresponding Author: ahmad.zaki@umy.ac.id
DOI: https://doi.org/10.30880/ijie.2024.16.01.031

Abstract

Concrete is one part of an infrastructure that is very commonly used, materials widely used in concrete, such as sand and gravel, come from nature that are limited and will run out if used continuously. Oil palm shell (OPS) waste is an alternative that can be used to solve this problem. In this study, the proportion of OPS used was 0%, 25%, 50%, and 75% as a partial substitute for coarse aggregate. Pre- and post-corrosion specimens use beam sizes with dimensions of 100 mm × 100 mm × 500 mm. The specimen has a corrosion rate of 7%. The specimen is tested for flexural strength, in addition, the specimen is tested using the Non-Destructive Testing (NDT) method at the age of 28 days and after acceleration corrosion. The NDT methods used in this study were resistivity and impact-echo as evaluation tools for the influence of OPS and fiber on corroded concrete. Based on the results, the lowest value of resistivity was 10.87 kohm/cm on 0% OPS post-corrosion specimen, and the highest value of resistivity of 24.12 kohm/cm on 0% OPS pre-corrosion specimen. Meanwhile, the impact-echo test obtained the lowest value of 2625.33 kHz on 75% OPS post-corrosion specimens and the highest impact-echo value of 11725.26 kHz on 0% OPS post-corrosion specimens. With the increase in the percentage of OPS, the resistivity obtained in pre-corrosion concrete will decrease as well as the impact echo value, except for the 75% OPS specimen, while in post-corrosion specimen impact-echo and resistivity are inversely proportional. The greater the percentage of OPS in concrete, the resistivity value tends to increase but the frequency of impact-echo tends to decrease except in specimens with 75% OPS.

1. Introduction

Infrastructure development that continues to grow yearly also affects the supply of existing materials. This is the background of the need to review using normal concrete material mixtures such as gravel and sand. This is because materials such as gravel and sand from nature are limited and will run out someday if they continue to be used in large quantities without renewal or replacement [1]. In this case, it is necessary to have an alternative innovation to replace the materials. Oil palm shell (OPS) is one of the alternative materials to replace the gravel [2]. Indonesia is the country with the largest oil palm plantation in the World [3]. In 2018, the area of oil palm plantations in Indonesia reached 14.3 million hectares [4]. Increasing oil palm production will cause the volume of waste from oil palm to increase over time because the process of recycling the waste produced is not optimal [5]. In this study, OPS partially replaced coarse aggregate for concrete mixtures. Many researchers investigate the physical and mechanical properties of concrete with OPS as an aggregate replacement [6]-[21]. According to Khan et al. [18], compressive strength decreases as the percentage of OPS in concrete increases. Therefore, fibre is needed to strengthen the concrete [6], [22], [23].

During the COVID-19 pandemic in Indonesia, the Ministry of Environment and Forestry Republic of Indonesia noted an increase waste from medical in the 30%–50% range. Medical waste was estimated at around 2,000 tons in 2020 [24]. In addition, according to Sangkham [25], Indonesia is ranked the 9th largest medical waste-producing country in the world, with 420.03 tons/day. They are adding a mask as fibre makes it possible to strengthen the concrete. In this study, mask fibres were used for concrete mixtures. The mask has polypropylene fibre in the material and can help increase the tensile strength of concrete [26]-[28]. According to Zhang et al. [29], polypropylene fibre is commonly used to manufacture nanofibers because the fibre has high tensile strength. Therefore, polypropylene fibre from mask waste is used as additional concrete mix material to increase the concrete's strength. Environmental conditions such as seawater can cause degradation to concrete quality, especially in Indonesia, where most of the country is seawater [30]. Indonesia has a seawater stretch area of approximately 5.8 million km^2 and a coastline of 95,181 km. It is the country with the longest coastline in the world [31]. Chloride concentration in seawater is *usually prohibited in* reinforced concrete (RC) structures, which can accelerate steel reinforcement corrosion [32]. Seawater has corrosive properties that can diffuse and erode the passive layer of steel reinforcement through the concrete pores, decreasing the concrete's durability [33], [34]. On the other hand, polypropylene fibre is resistant to chemical and alkaline reactions due to seawater [35]. Although using polypropylene fibre could reduce water absorption in concrete [36], [37], the research that uses OPS and polypropylene fibre as concrete material in seawater environments is limited [35].

The effect of steel reinforcement corrosion on RC needs to be evaluated with an inspection method so that RC can be repaired or maintained before it does not function properly because it is damaged by steel corrosion [38]. In a corroded RC structure, the volume of the corrosion product (rust) can be greater than three times the volume of the original steel reinforcement material, resulting in cracks in concrete [39]. This is the beginning of RC damage, which can eventually lead to more severe damage, thus shortening the life of the building in question. Therefore, the non-destructive testing (NDT) method will be used as an inspection method to evaluate the condition of OPS fibre-concrete in a corrosive environment. The NDT methods used in the study are resistivity and impact echo. The ultrasonic pulse velocity (UPV) of NDT methods [40]-[44] has been studied to evaluate the OPS fibre-concrete. However, there is a limited study on OPS-fibre concrete for other NDT methods, especially when considering OPS-fiber concrete with steel reinforcement. Hence, this study aims to determine the feasibility of using resistivity and impact echo for evaluating the steel corrosion of the fibre-concrete in pre-corrosion and post-corrosion specimens with different percentages (%) of OPS as aggregate replacement.

2. Research Methodology

The materials used in the concrete mix are Portland cement, water, fine aggregate, coarse aggregate, OPS, and polypropylene fibre from the medical mask. The maximum size used for gravel and OPS is 20 mm with specific gravity of 1.39 and 2.68, respectively, and the size of the sand used is 0.0075 mm to 4.8 mm. The polypropylene fibre is 20 mm long by 5 mm wide. The OPS and Polypropylene fibre are shown in Fig. 1.
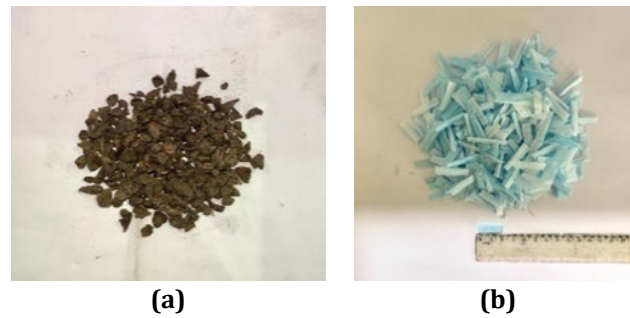
Fig. 1 *(a) OPS; and (b) Polypropylene fibre*

The mix design of 30 MPa concrete refers to SNI 03–2834–2000 [45]. There were variations by replacing some gravel with OPS with percentages of 0%, 25%, 50%, and 75%, and there was an added material in the form of polypropylene fibre of 0.2% and superplasticizer (SP) of 0.25%. The mix design in the study used a water content of 0.48. The mix design is shown in Table 1. The specimen used in this study consisted of a cylinder with a diameter of 750 mm and a height of 150 mm for the compressive strength test and a beam specimen for the flexural strength test. The 24 concrete beam specimens are 100 mm × 100 mm × 500 mm, with three beams at each % of OPS. The beam dimensions are shown in Fig. 2.

Table 1 *Mix design in kg/m³*

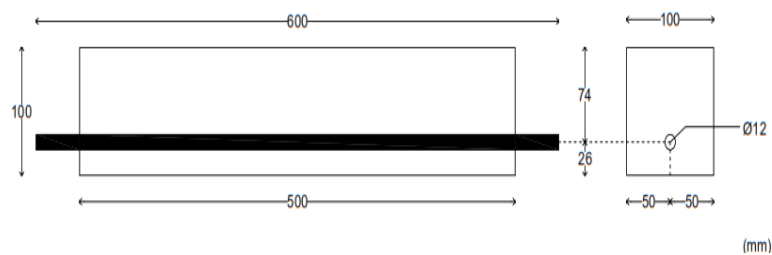| Mixture ID	OPS (%)	Water (L/m³)	Cement (kg/m³)	Gravel (kg/m³)	Sand (kg/m³)	OPS (kg/m³)	Fibre (kg/m³)	SP (kg/m³)
C	0	204.9	426.86	944.85	698.37	0,00	0.0273	1.065
OPS25	25	204.9	426.86	708.64	698.37	236.21	0.0273	1.065
OPS50	50	204.9	426.86	472,42	698.37	472.86	0.0273	1.065
OPS75	75	204.9	426.86	236.21	698.37	708.64	0.0273	1.065

Fig. 2 *Dimensions of beam specimen (in mm)*

In this study, wet burlap sack curing was the 28-day curing method. Two are pre-corrosion specimens (accelerated steel reinforcement before concrete casting) and post-corrosion specimens (accelerated steel reinforcement after concrete casting). The slump value obtained is the same for each specimen variation. For pre- and post-corrosion specimens, the slump value was measured at around 100-125 mm. The corrosion process uses the acceleration corrosion technique with the impressed current technique using a DC power supply based on ASTM G1-03 [46] and ASTM G31-72 [47], as shown in Fig. 3(a). The positive pole is connected with the reinforcement in concrete as the anode. In contrast, the negative pole, the external reinforcement, is the cathode. The boxes containing 5% NaCl solution immerse the concrete specimen. It can be calculated using Faraday's Law [48]. The concrete beam specimen has been corroded for 7% of the corrosion level (mass loss). Non-destructive testing (NDT) methods are carried out at 28 days of concrete age. NDT testing is carried out before and after corrosion of steel reinforcement, i.e., resistivity and impact-echo techniques, as shown in Fig. 3(b) and Fig. 3(c). After a 28-day curing process and NDT, flexural strength testing was carried out using a Universal Testing Machine (UTM) with the Hung Ta brand. The flexural strength testing can be seen in Fig. 3(d).
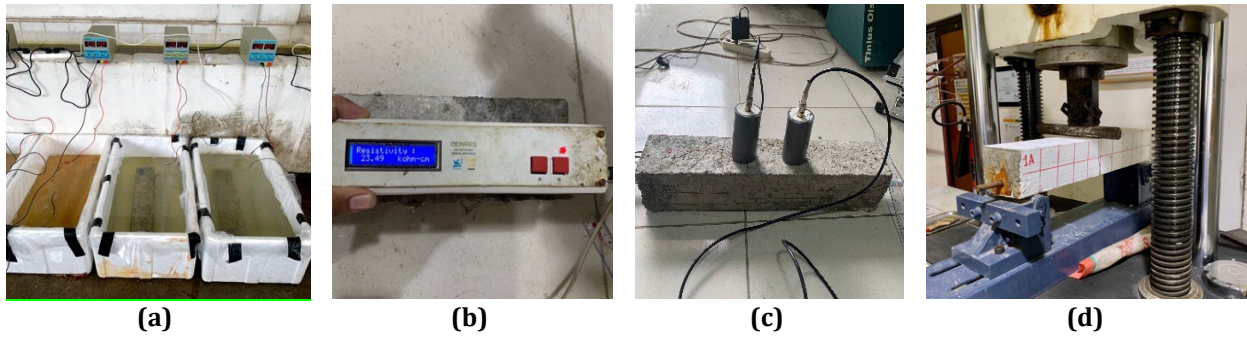
Fig. 3 *Testing of beam specimen: (a) Accelerated corrosion; (b) Resistivity; (c) Impact-Echo; and (d) Flexural strength*

Fig. 4(a) gives details of the division of the side, which is the area tested from the resistivity technique, used the division of sides into three parts intending to get the best and even results so that they are evenly obtained from the three sides. On the other hand, Fig. 4(b) gives details of the placement of the hit point and the placement of 2 sensors of Impact Echo (IE) as wave receivers. Placement is used as in the picture above to maximize the results obtained through good wave data.
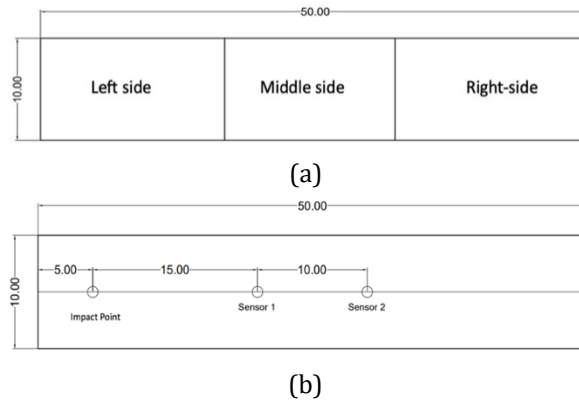

(a)

(b)

Fig. 4 *Test schematic of beam specimen: (a) Resistivity testing; and (b) Impact-echo testing*

3. Results and Discussion

3.1 Testing of Materials

There are several tests on aggregates, namely testing specific gravity and water absorption, fill weight, moisture content, and sludge content, for coarse aggregate and OPS, and fine grain modulus (MHB) testing, specific gravity, water absorption, fill weight, moisture content, and sludge content, for fine aggregate. The test results can be seen in Table 2. Gradation testing on the fine aggregate (sand) was carried out based on SNI ASTM C136:2012 [49]. The sand used in this test obtained an MHB value of 2.38 and entered the gradation of area 2. The area was a bit of coarse sand. From the test results, the MHB (Fine Modulus of grains) value has met the criteria in the range of 1.5 to 3.8. In making concrete, it is necessary to test the workability to determine the viscosity of the concrete mixture with the condition that the slump is between 75 – 150 mm.

Table 2 *Test results of coarse aggregates, OPS, and fine aggregate*

Types of Testing	Gravel	OPS	Sand	Unit
Specific Gravity	2.68	1.20	2,27	-
MHB	-	-	2,38	-
Water Absorption	1	16.25	2,57	%
Fill Weight	1.49	0.64	1.52	gram/cm^3
Air Up	0.83	3.36	2	%
Mud Rate	1	1	2	%
Wear	29	5.5	-	%

3.2 Density

Density is a derivative quantity because it includes units of mass (kg) and volume (m³). This density test is carried out to determine the density level of concrete every 1 m³. The way to test the density of concrete is to compare the mass of concrete (kg) with the volume of the specimen (m³). The cylinder specimen used is cylindrical with a diameter and height of 75 mm and 150 mm, so the specimen volume value is 0.000663 m³. The density of cylinder specimens is 2336.47 kg/m³, 2208.21 kg/m³, 2120.18 kg/m³, and 1954.19 kg/m³, for C, OPS25, OPS50, and OPS75, respectively. For the beam specimen, the specimen used is a beam with a specimen volume value of 0.005 m³. Table 3 is the density chart of the pre-and post-corrosion specimens. Every % OPS has three beam specimens.

Table 3 *Average density value of the specimens*

Mixture ID	Pre-corrosion (kg/m³)	Post-corrosion (kg/m³)
C	2417	2337
OPS25	2250	2240
OPS50	2117	2097
OPS75	1930	1963

Table 3 shows that the density of pre-corrosion concrete decreases with the increase of OPS content. The average density value of the specimens is 2417 kg/m³, 2250 kg/m³, 2117 kg/m³, and 1930 kg/m³ for C, OPS25, OPS50, and OPS75, respectively. On the other hand, post-corrosion specimens have density values of 2337 kg/m³, 2240 kg/m³, 2097 kg/m³, and 1963 kg/m³ for C, OPS25, OPS50, and OPS75, respectively. The density results show that the higher the content of OPS, the lower the density value of the concrete specimen. This happens because the alternation of coarse aggregates with OPS leads to a decrease in the weight of concrete. According to Shafigh et al. [50] in their research, the density of OPS concrete is approximately 20 to 25% lower than normal concrete.

3.3 Compressive Strength

Table 4 shows the compressive strength values for each cylinder specimen. For the control specimen, the strength did not achieve the design strength of 30 MPa. The polypropylene fibre makes bonding strength between the fibre and the concrete matrix poor due to the smooth surface of the fibre. The compressive strength value decreased in terms of an increase of % OPS. The decrease was 33.2%, 36.69%, and 54.75% compared to the 0%-cylinder specimen. This is due to the high-water absorption due to the increasing percentage of OPS. Still, the percentage of SP used cannot support and maintain the proportion of water so that the material is not mixed evenly, and the bond between materials is reduced. According to Azunna [17], the decrease in the compressive strength of concrete is due to the lack of bonds between concrete particles. This is because particle bonding largely depends on the surface texture, whereas the cement paste bond is more adequate with rough surfaces.

Table 4 *Average compressive test of the specimen*

Mixture ID	Compressive Strength (MPa)
C	15.63
OPS25	14.78
OPS50	10.32
OPS75	9.78

3.4 Load-Deflection

Fig. 5(a) is a load-deflection graph of all pre-corrosion specimens. From the load-deflection value that has been obtained, it can be concluded that the greater the percentage of OPS, the load-deflection value on the concrete decreases. This happens because the stiffness of the concrete influence's concrete deflection; the higher the rigidity of concrete, the higher the deflection value obtained.
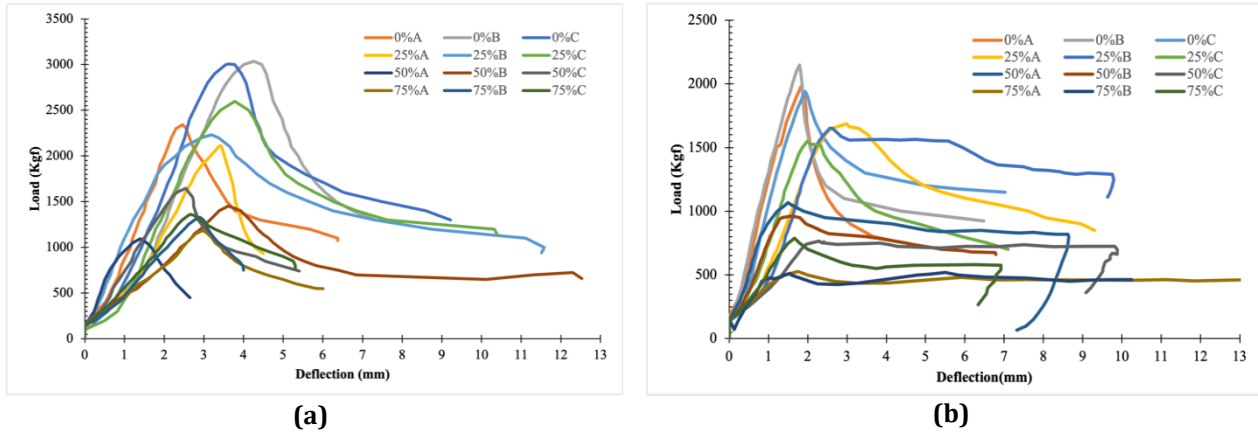
Fig. 5 *Load and deflection of: (a) Pre-corrosion specimens; and (b) Post-corrosion specimens*

Ductility in specimens can be calculated by comparing the value between ultimate deflection and deflection when melting, as shown in Table 5. Table 5 shows that with the increase in the percentage of OPS on concrete, the ductility value of concrete decreases, although it does not show a significant reduction. This is because the ductility value is influenced by steel reinforcement and the addition of fibres. According to Orouji et al. [51], large ductility causes the energy absorbed to be greater so that the deflection becomes greater due to the influence of the amount of fibre composition mixed in concrete. However, OPS25 specimens with 25% OPS have a higher ductility value of 1.359 than others. This happens because the OPS25 specimen is more ductile than other specimens. The high ductility could be caused by OPS25 specimens having a corrosion influence on different reinforcements and the influence of mask fibres. According to Naderpour et al. [52], corrosion reduces the load that can be carried by beam specimens by decreasing the ability of beam specimens to withstand loads, resulting in a reduction in area or cross-section, which affects the performance of reinforcement in carrying the resulting load, including affecting ductility. The specimen's stiffness can be calculated by dividing the modulus of elasticity by the unit voltage received by the change in the shape of the unit, as shown in Table 5. Table 5 shows that with the increase in the percentage of OPS on concrete specimens, the rigidity value of concrete specimens decreases. This happens because OPS used as an aggregate substitute has a lower hardness than gravel. According to Shafigh et al. [53] stated that the stiffness value is influenced by the aggregate hardness used. Of all specimens, the highest average stiffness value of 9.697 kN/mm occurred in concrete specimens with C specimens. The lowest average stiffness value was 4.857 kN/mm in OPS75 concrete specimens.

Table 5 *Average ductility and stiffness of pre-corrosion specimen*

Mixture ID	Ductility	Stiffness
C	1.198	9.697
OPS25	1.359	8.973
OPS50	1.123	6.743
OPS75	1.108	4.857

On the other hand, Fig. 5(b) shows a graph of the load-deflection relationship of OPS post-corrosion specimens. Based on the results below, the highest deflection value was obtained by a 75%A specimen of 12.53 mm with an ultimate load of 527.08 Kgf. A 0%A specimen of 4.064 mm obtained the lowest deflection value with a maximum load of 1981.1 Kgf. From this result, it can be concluded that the higher the percentage of OPS mixture, the deflection value in concrete tends to decrease. Ductility is the ability of materials in concrete to develop their stretch from the first time it melts until it finally breaks. Ductility can be calculated using the ratio between deflection when ultimate and deflection when melting. Table 6 shows the ductility value of the OPS concrete test specimen at a corrosion level of 7%.

Table 6 *Average ductility and stiffness of post-corrosion specimen*

Mixture ID	Ductility	Stiffness
C	1.198	9.697
OPS25	1.149	7.427
OPS50	1.311	7.350
OPS75	2.983	4.967

Table 6 shows that, in general, the increase in the percentage of OPS causes an increase in the ductility value in concrete, and in OPS75 specimens, there is a high ductility value. This is because adding mask fibres to the concrete mix has an effect that causes large deflections [51]. According to research conducted by Hosen et al. [54] and Cui et al. [55], adding OPS and mask fibres to concrete can increase the energy absorption ability of the mixed matrix, which means the ductility value has increased. Stiffness is the quotient between the load and deflection from the flexural strength test results. The stiffness values, as shown in Table 6, show that with an increasing percentage of OPS on concrete, the stiffness values in concrete decrease. The specimen with the highest average stiffness value of 9.697 kN/mm in concrete with a combination of 0% OPS, while the specimen with the lowest stiffness value has an average stiffness value of 4.967 kN/mm in concrete with a mixture of 75% OPS. The stiffness value is controlled by the aggregate hardness used [53].

3.5 Flexural Strength

Specimens completed with corrosion processes, both pre-corrosion and post-corrosion specimens, will then be tested for flexural strength using a Universal Testing Machine (UTM), as shown in Fig. 6. The specimen was carried out using one loading point in the middle of the beam span with a distance between the pedestal and the edge of the beam of 5 cm. This test was carried out to determine the effect of the difference in the percentage of OPS on corroded fibre concrete. Fig. 6(a) and Fig. 6(b) show that as the mixture of OPS increases in concrete, the value of the flexural strength of concrete decreases. For the pre-corrosion specimen, the highest average flexural strength value is in concrete with a 0% OPS mixture of 2.74 MPa, while the lowest average flexural strength value is in concrete with a 75% OPS mixture of 1.27 MPa. For the post-corrosion specimen, the highest average flexural strength value is in concrete with a 0% OPS mixture of 1.98 MPa, while the lowest average flexural strength value is in concrete with a 75% OPS mixture of 0.60 MPa. This is because one thing that affects the strength of concrete is the aggregate quality. In this study, the aggregate is replaced with OPS, so adding OPS will decrease the strength of concrete. Study conducted by Kareem et al. [56] also showed that adding OPS will reduce the strength of concrete. In addition, when compared with pre-corrosion specimens, the post-corrosion specimens are inferior in flexural strength. This is because the acceleration of the corrosion process of reinforced concrete structures has repercussions regarding serviceability.
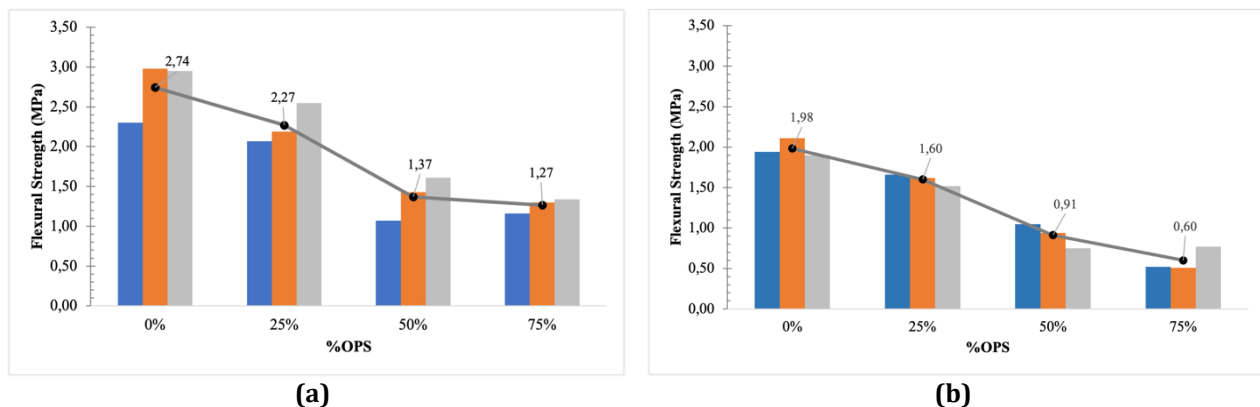

| (a) | (b) |

Fig. 6 *Flexural strength of: (a) Pre-corrosion specimen; and (b) Post-corrosion specimen*

3.6 Failure Type

3.6.1 Pre-corrosion Specimen

In addition to the value of flexural strength, the failure of the specimen is checked based on the location of the cracks due to the test. The crack's direction and the crack's location in the beam are used to classify the type of failure. Fig. 7 to Fig. 10 show the collapse pattern on the almost concrete specimen is a type of diagonal tensile crack because there is a fine crack in the centre of the span caused by flexural, followed by a diagonal crack extending from the area around the pedestal to the centre of the span.
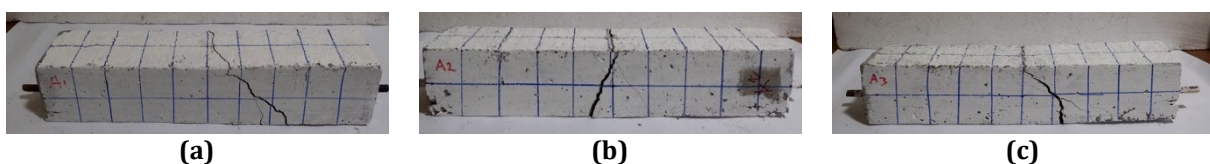

| (a) | (b) | (c) |

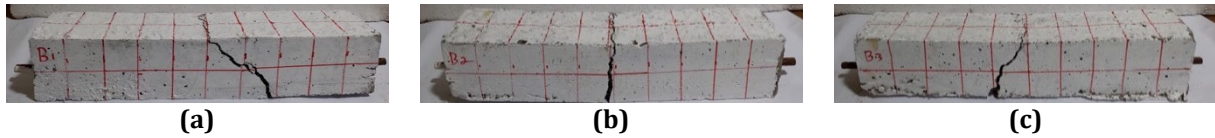**Fig. 7** *Failure type of pre-corrosion specimen with 0%OPS*

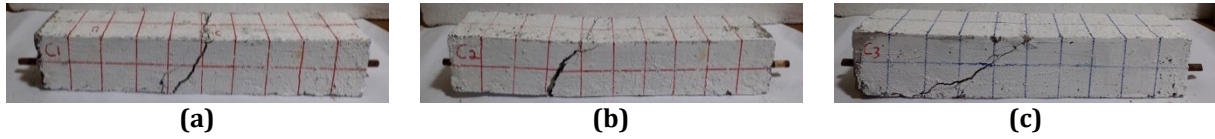**Fig. 8** *Failure type of pre-corrosion specimen with 25%OPS*

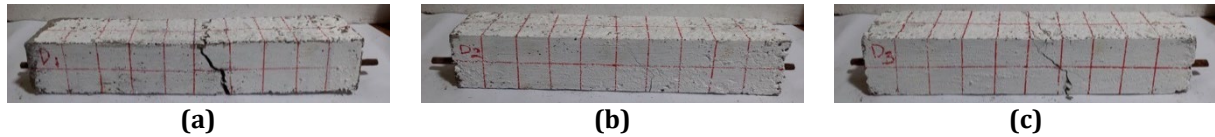**Fig. 9** *Failure type of pre-corrosion specimen with 50%OPS*

Fig. 10 *Failure type of pre-corrosion specimen with 75%OPS*

3.6.2 Post-corrosion Specimen

Fig. 11 to Fig. 14 show concrete specimen failure during flexural strength testing of OPS fibre-concrete that is corroded. In beam (b), a diagonal tensile collapse occurs because of a small crack in the centre of the span caused by bending, followed by a diagonal crack extending from the pedestal area to the centre of the span. Meanwhile, due to perpendicular cracks in the centre of the beam, beams (a) and (c) experience a pattern of bending collapse. Fig. 12 shows concrete beams collapsing during flexural strength testing due to a mixture of 25% OPS. Beams (a), (b), and (c) experience the same collapse, namely bending failure, due to perpendicular cracks in the centre of the beam. Fig. 13 shows a concrete specimen collapsing during flexural strength testing due to a mixture of 50% OPS. Beams (a), (b), and (c) experience the same collapse, namely bending failure, due to perpendicular cracks in the centre of the beam. Fig. 14 shows a concrete specimen collapsing during flexural strength testing due to a mixture of 75% OPS. In beam (a), there is a bending collapse due to perpendicular cracks in the center of the beam. In beam (b), there is a diagonal tensile collapse because of a small crack in the middle of the span caused by bending, followed by a diagonal crack extending from the fulcrum area to the center of the span. Meanwhile, due to the crack tilted towards the middle of the span and the location of the crack in the middle of the span due to pressure from the pedestal that occurs on the beam (c), it experiences a pattern of sliding compressive collapse.
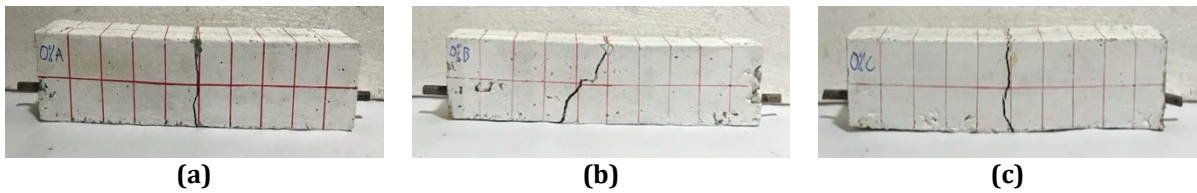

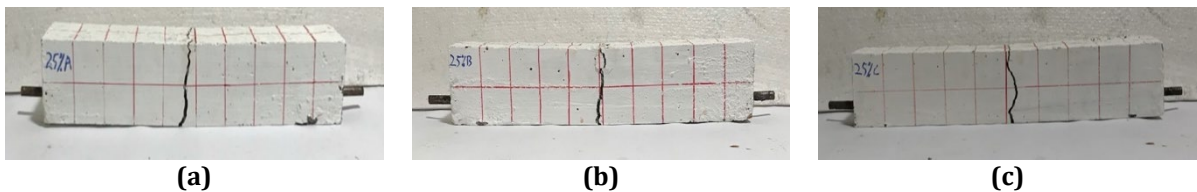**Fig. 11** *Failure type of post-corrosion specimen with 0%OPS*

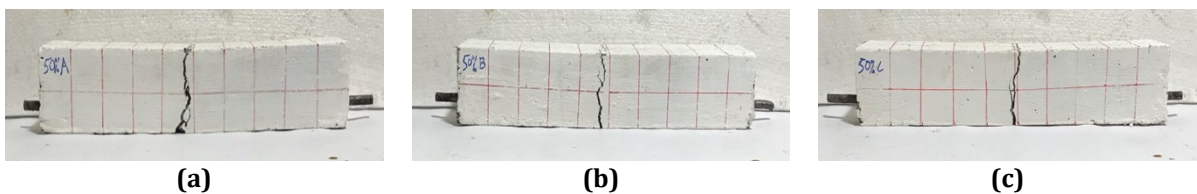**Fig. 12** *Failure type of post-corrosion specimen with 25%OPS*

Fig. 13 *Failure type of post-corrosion specimen with 50%OPS*

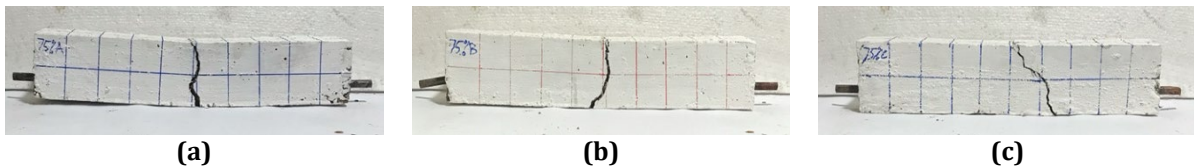| (a) | (b) | (c) |

Fig. 14 *Failure type of post-corrosion specimen with 75%OPS*

3.7 NDT Method

3.7.1 Resistivity

Resistivity testing is an NDT method to determine the corrosion level contained in the specimen, i.e., pre-corrosion and post-corrosion specimens. Resistivity testing is done by determining 3 test points on the specimen to get even more accurate results. Therefore, 3 points are determined, namely at the right end, the middle, and the left end of the specimen, by repeating the test 3 times to get accurate results. The results are then summarized in a picture as a bar chart showing the difference of each variation of the OPS of 0%, 25%, 50%, and 75%. These results can be seen in Fig. 15 and Fig. 16. Fig. 15 shows the resistivity of the pre-corrosion specimen. The resistivity value of 10-50 kΩ/cm indicates a moderate risk of exposure to corrosion risk. In addition, with the increased percentage of OPS on concrete, the resistivity value obtained is lower. This states that the higher the percentage of OPS used, the smaller the resistance because concrete is not as homogeneous as concrete with gravel alone. This is due to the vast percentage of water absorption of OPS, which will later cause the concrete to lack water so that it will not be completely homogeneous and become more porous due to many pores [57].

Fig. 16 shows the resistivity of post-corrosion specimens before and after corrosion. The figure shows that with the increase in the percentage of OPS on concrete, the resistivity value obtained is also higher. This indicates that the greater the percentage of OPS used, the smaller the corrosion level in concrete. This is different from the resistivity of the pre-corrosion specimen. However, the resistivity value is still in the same risk range of 10-50 kΩ/cm, which indicates a moderate risk of exposure to corrosion risk. The figure shows that as the mixture of OPS increases in concrete, the resistivity value is also higher. This explains that the percentage of OPS, regardless of the proportion, is insignificant, causing a higher risk of corrosion in this specimen. In addition, the resistivity of all specimens is close to the value of <10 kΩ/cm, which indicates a high risk due to corrosion [58], [59]. Fig. 16 (c) shows the average value of resistivity test results on post-corrosion specimens before and after corrosion. From the figure, it was found that after corrosion was carried out, the resistivity value obtained was reduced compared to the specimen before corrosion. This indicates that corrosion significantly affects the resistivity value of the specimen. It is explained that the specimen after corrosion is included in the moderate group of corrosion risks range of 10-50 kΩ/cm.
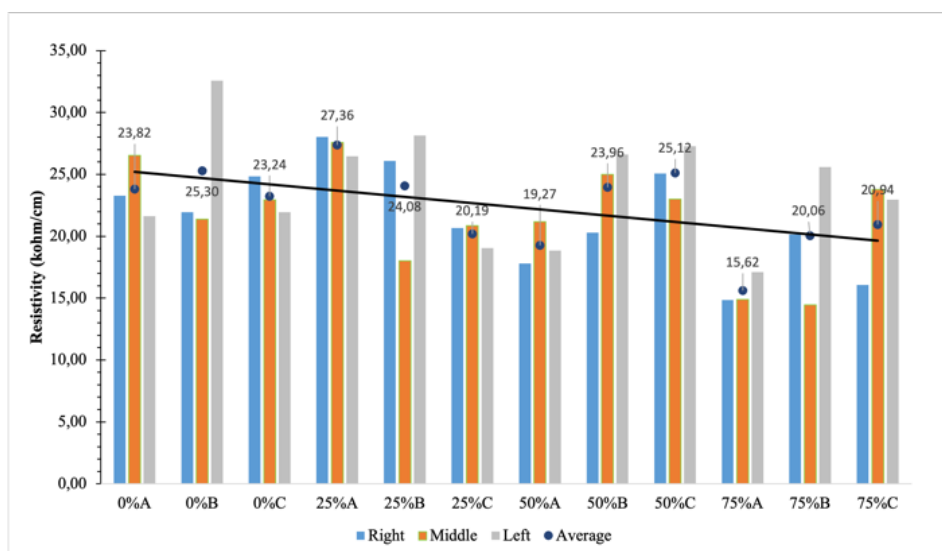

Fig. 15 *Resistivity of pre-corrosion specimen*
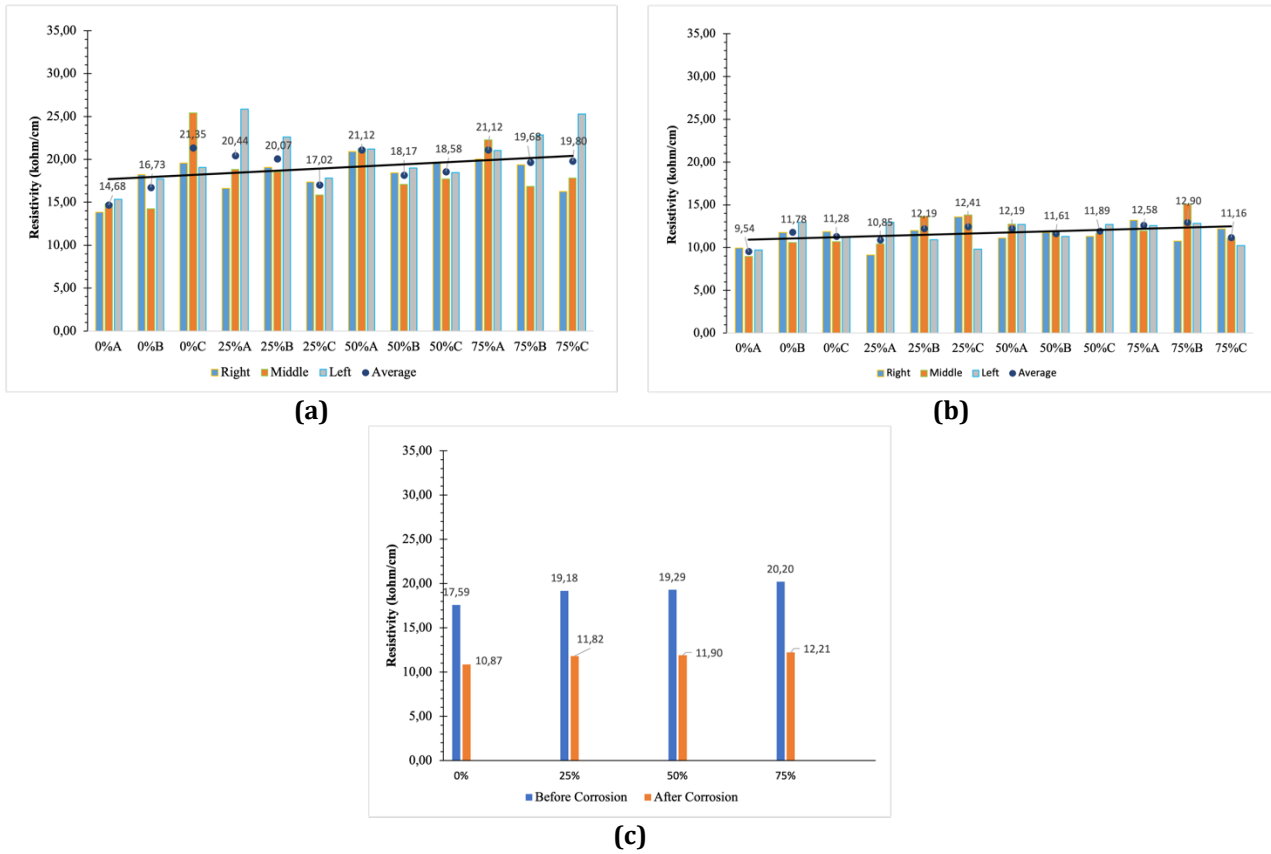
(a)

(b)

(c)

Fig. 16 *Resistivity of Post-corrosion specimen: (a) before corrosion; (b) after corrosion; and (c) comparison*

Based on the relationship between resistivity and density, in pre-corrosion specimens, the more significant the density value, the greater the resistivity value, but in post-corrosion specimens, different results are obtained, namely, the greater the density value, the smaller the resistivity value. This is strengthened by the research of Golewsky [60] which states that corrosion is the cause of decreasing density in concrete because it causes a reduction in the area of the paired reinforcement, causing the creation of cavities that will have an impact on the strength of the concrete. These results can be seen in Fig. 17 and Fig.18.

Fig. 19 shows the relationship between resistivity and flexural strength of pre-corrosion specimens. It is explained that in the pre-corrosion specimen (Fig. 19(a)), the resistivity value and the flexural strength value decrease with the increase in the percentage of OPS. However, in the post-corrosion specimen, different results were obtained, namely, the value of flexural strength decreases with the increase in the resistivity value. The resistivity value is still not much different and is in the same corrosion risk range of 10-50 kΩ/cm, indicating a moderate risk of exposure to corrosion risk [58].
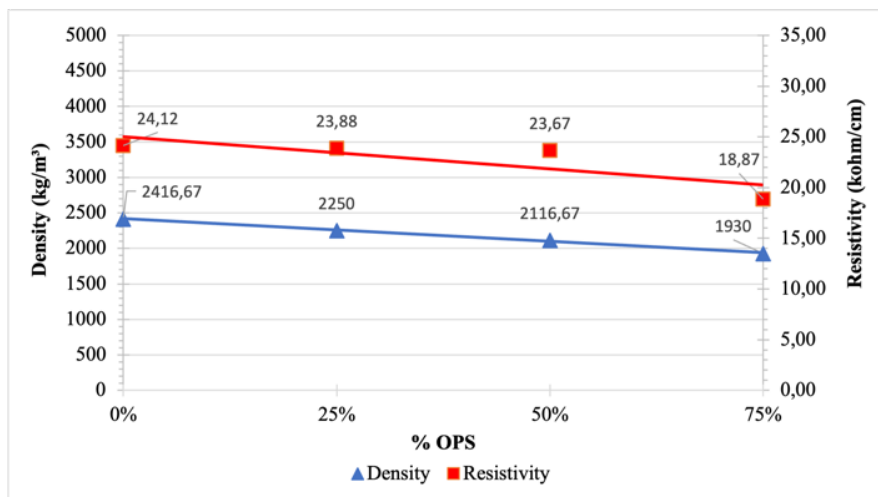

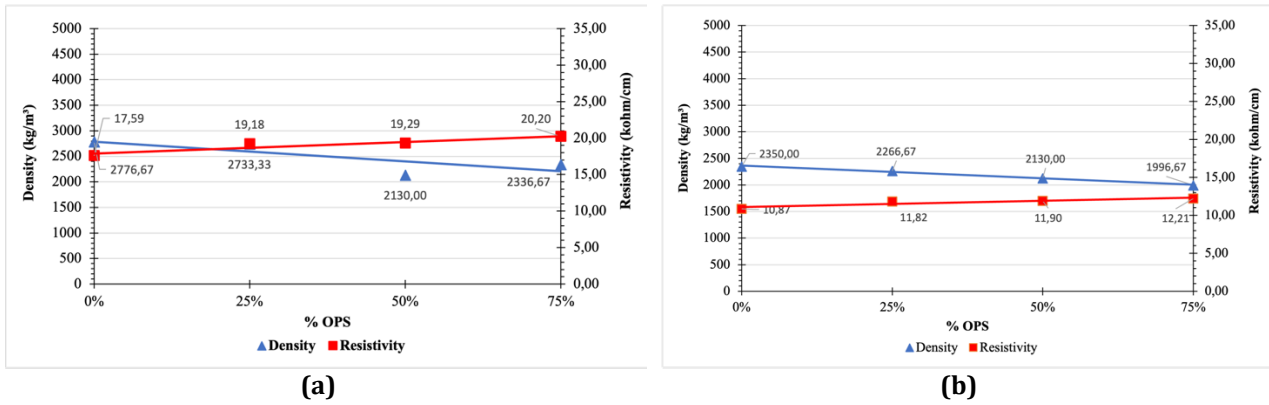**Fig. 17** *Resistivity and density of pre-corrosion specimen*

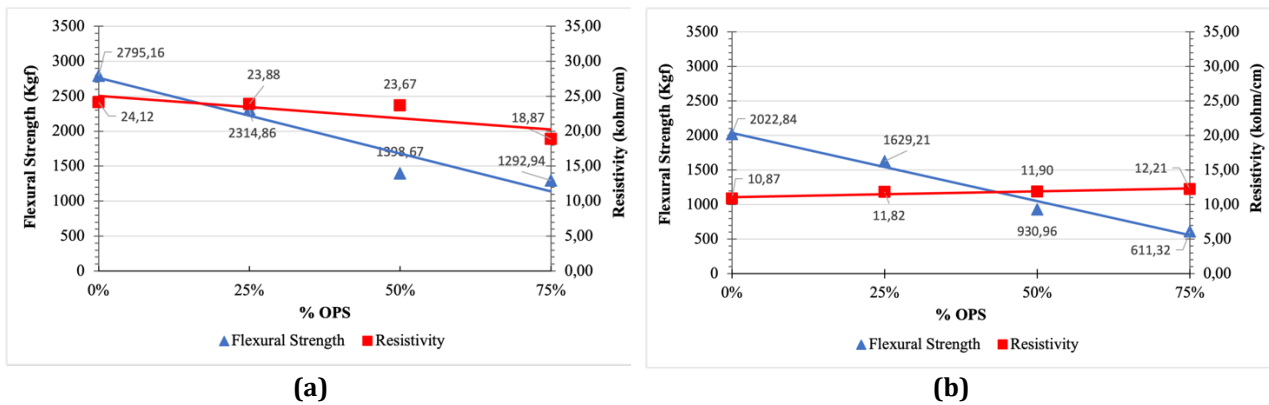**Fig. 18** *Resistivity and density of post-corrosion specimen: (a) Before corrosion; and (b) After corrosion*

Fig. 19 *Resistivity and flexural strength of: (a) Pre-corrosion specimen; and (b) Post-corrosion specimen*

3.7.2 Impact Echo Testing

Impact-echo testing is a test that utilizes the principle of waves that can propagate through solid objects and can be reflected. From this principle, testing is carried out in the form of wave utilization to determine the concrete condition without the need to damage the physical shape of the concrete and affect its compressive strength. This test uses two sensors to capture the waves of a blow at a predetermined point. The results are in the form of various frequencies that produce the peak of an amplitude with a specific value that is a deviation from the value of another amplitude. Impact Echo testing in this study was carried out as many as three repetitions on each specimen to get better and more accurate results. Fig. 20 is the graph of impact echo results of the pre-corrosion specimen.
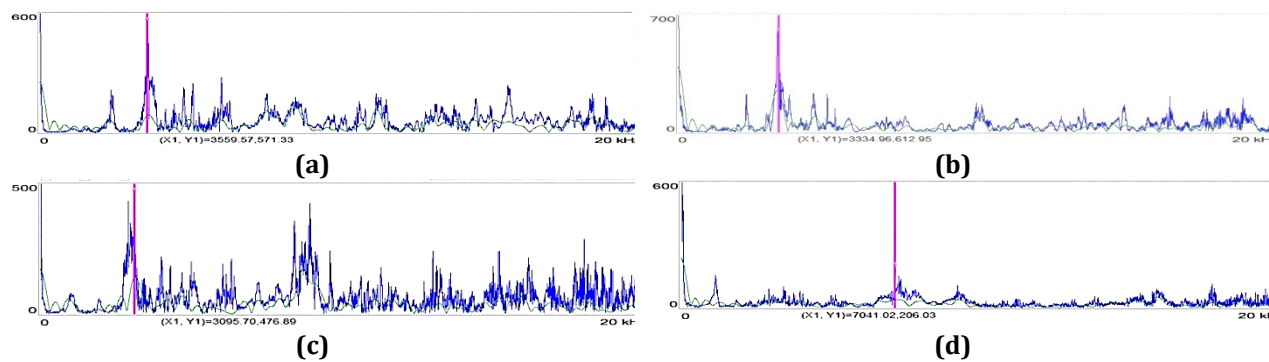

Fig. 20 *Impact echo results of the pre-corrosion specimen: (a) 0% OPS; (b) 25% OPS; (c) 50% OPS; and (d) 75% OPS*

Fig. 21 is a pre-corrosion specimen where the frequency value of impact-echo decreases with an increasing percentage of OPS. This is because the higher the percentage of OPS, the smaller cavities or gaps are formed that can affect the propagation of waves delivered in the impact-echo test [61]. In Fig. 21, the graph has a correlation coefficient 0.4051 between -1 and 1. If the value is close to -1 or 1, then the correlation between the variables studied is strong, and if the value is close to 0, it means a weak correlation. So, it was concluded that the percentage

of OPS and the frequency of impact echoes correlated but were relatively weak (close to 0) in the pre-corrosion specimen.
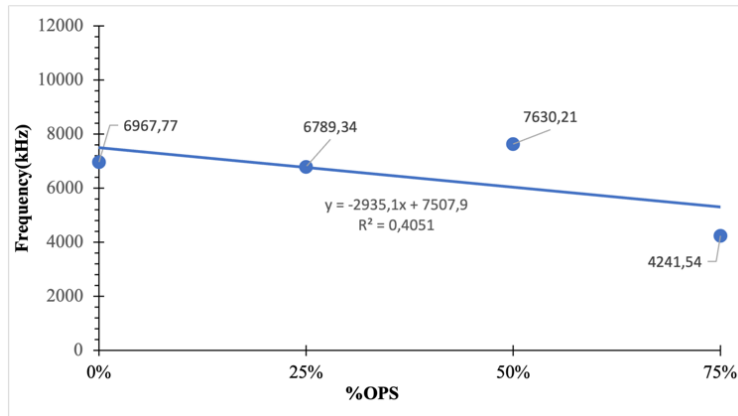

Fig. 21 *Impact echo frequency of pre-corrosion specimen*

Fig. 22 is the graph of impact echo results of the post-corrosion specimen. Fig. 23 of the post-corrosion specimen, the impact echo frequency value decreases with increasing percentage of the OPS, except in special post-corrosion OPS of 75%. This is because the higher the percentage of OPS, the smaller cavities or gaps are formed that can affect the propagation of waves delivered in the impact-echo test [61]. The graph has a correlation coefficient of 0.0108 and 0.2263, between -1 and 1. If the value is close to -1 or 1, then the correlation between the variables studied is strong, and if the value is close to 0, it means a weak correlation. So, it was concluded that the percentage of OPS and the frequency impact-echo correlated but were relatively weak in post-corrosion specimens.
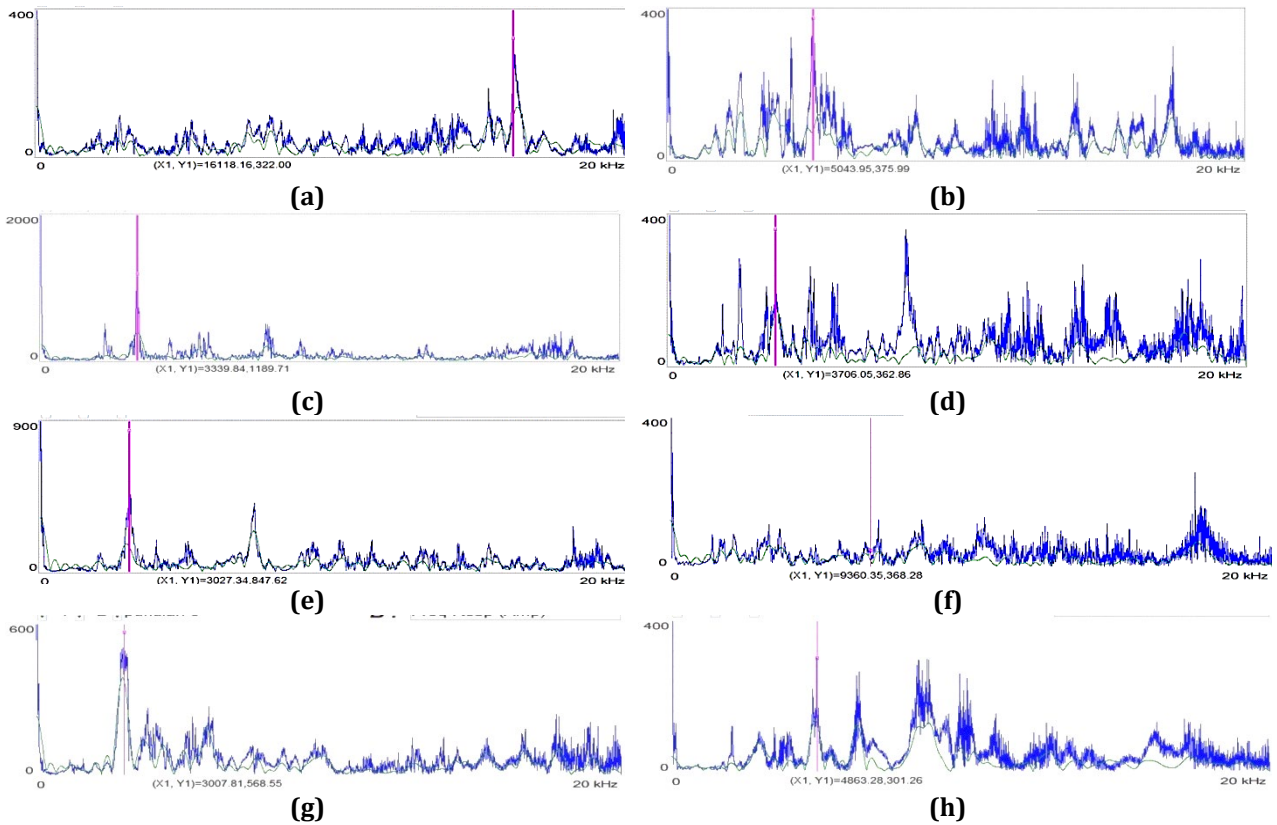

Fig. 22 *Impact echo results of the post-corrosion specimen: (a) 0% OPS before; (b) % OPS after; (c) 25% OPS before; (d) 25% OPS after; (e) 50% OPS before; (f) 50% OPS after; (g) 75% OPS before; and (h) 75% OPS after*
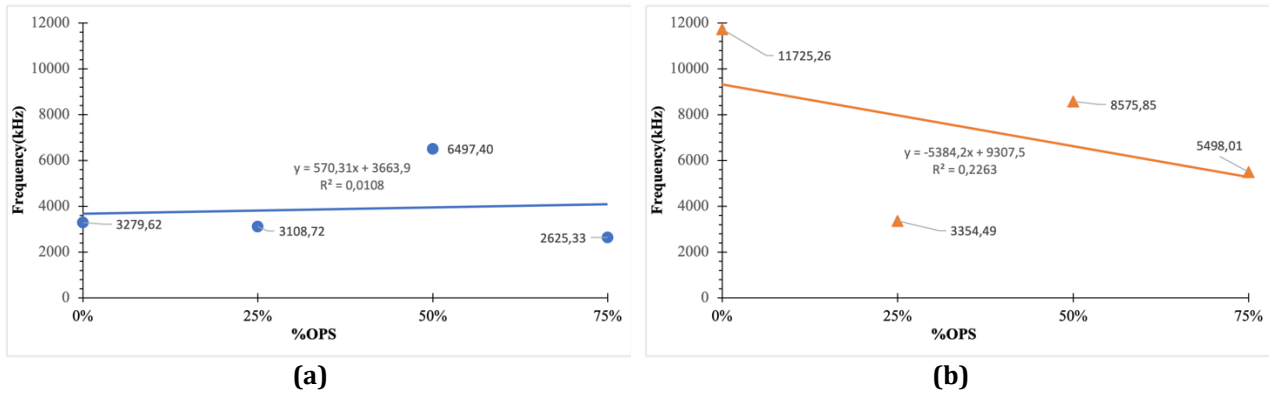
Fig. 23 *Impact echo frequency of post-corrosion specimen: (a) before corrosion; and (b) after corrosion*

Fig. 24 shows impact-echo testing on post-corrosion specimens before and after corrosion. It can be seen in the picture below that after concrete undergoes acceleration corrosion, the value of the impact echo is higher than before the acceleration corrosion. This explains that corrosion increases the impact-echo frequency because, after the corrosion process, it causes the formation of cavities in concrete. This is reinforced by the research of Farhangdoust and Mehrabi [61] which states that corrosion can cause concrete to become hollow.
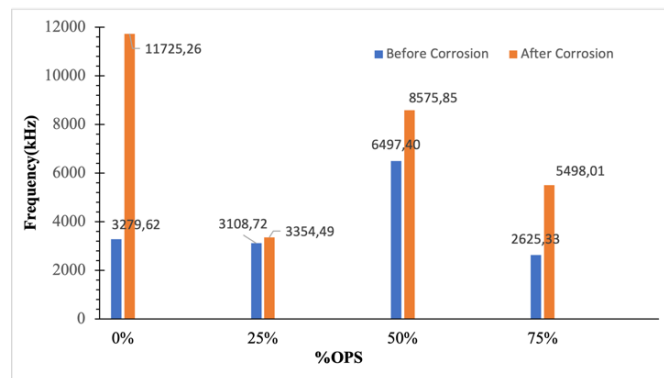

Fig. 24 *Comparison impact echo frequency of post-corrosion specimen before corrosion and after corrosion*

3.7.3 Comparison of Resistivity and Impact Echo Values

After resistivity and impact-echo testing on pre-corrosion and post-corrosion specimens, a comparison was made between the results of the two methods. In Fig. 25 on the pre-corrosion specimen, the relationship between impact-echo and resistivity is directly proportional. It can be seen in the figure below that the greater the percentage of OPS in concrete, the resistivity value and impact-echo frequency decrease, except for the specimen of 75% OPS. This explains that the large percentage of OPS will affect the resistivity and impact echo values because more cavities or pores occur, as described in the previous section.
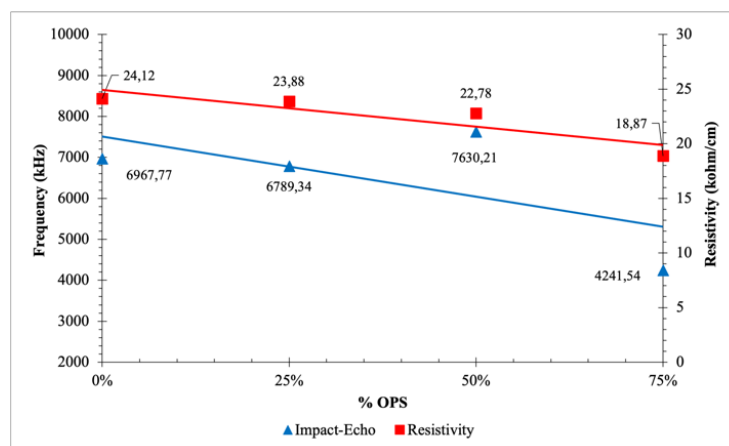

Fig. 25 *Comparison of resistivity and impact echo of pre-corrosion specimen*

In Fig. 26, the relationship between impact-echo and resistivity is inversely proportional to post-corrosion specimens before and after corrosion. It can be seen in the figure below that the greater the percentage of OPS in concrete, the resistivity value tends to increase, but the impact-echo frequency tends to decrease except for the specimen of 75% OPS. This explains that the large percentage of OPS does not decrease the resistivity value, which should reduce resistivity due to increasing OPS and corrosion. However, it affects the value of impact-echo because more and more cavities or pores occur, as described in the previous section.
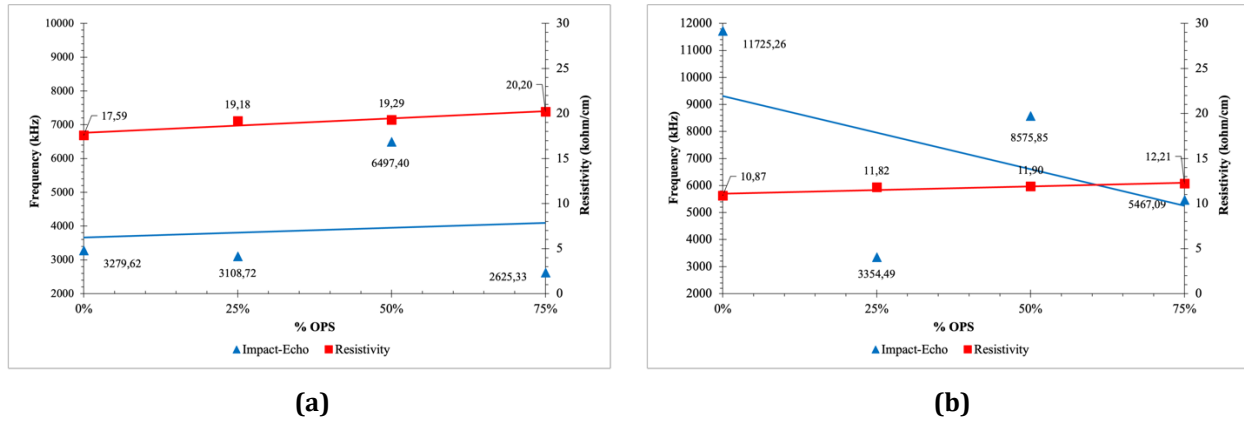

(a)   **(b)**

Fig. 26 *Comparison of resistivity and impact echo of the post-corrosion specimen: (a) before corrosion; and (b) after corrosion*

4. Conclusions

Based on the research results on concrete pre-corrosion and post-corrosion specimens with OPS and mask fibres, it can be concluded as follows:

- The results of resistivity testing on pre-corrosion specimens of OPS concrete and mask fibre showed that the greater the percentage of OPS, the lower the resistivity value. Meanwhile, in the post-corrosion specimen, the result is that the greater the percentage of OPS, the greater the resistivity value. This can be caused by the influence of OPS and the influence of corrosion on the specimen.
- The difference in resistivity of pre-corrosion and post-corrosion specimens: In pre-corrosion specimens, the resistivity value decreases with the increase in the percentage of OPS in concrete, while in post-corrosion specimens, the resistivity value increases with the increase in the percentage of OPS in concrete.
- The results of the impact-echo test on pre-corrosion and post-corrosion specimens of OPS and mask fibres show that a higher percentage of OPS makes the bending strength weaker because there are many cavities or pores in the concrete which will affect the bending strength of concrete.
- The difference between impact-echo pre-corrosion and post-corrosion specimens is that in pre-corrosion specimens, the value obtained ranges from 4000-8000 kHz, while in post-corrosion specimens, the value obtained ranges from 2000-12000 kHz.
- The effect of the relationship between density and bending strength with resistivity and impact-echo testing. The density of concrete decreases with the increase in OPS, causing the creation of cavities that will impact the strength of concrete, namely flexural strength.
- The relationship between resistivity and impact-echo testing on OPS concrete and corrosion mask fibres for pre-corrosion specimens is directly proportional, that the greater the percentage of OPS in concrete, the resistivity value and frequency of impact-echo decrease except for 75% OPS specimens. As for post-corrosion specimens, the relationship between impact-echo and resistivity is inversely proportional. The greater the percentage of OPS in concrete, the greater the resistivity value, but the frequency of impact-echo tends to decrease except for specimens with 75% OPS.

Acknowledgement

Conflict of Interest

Authors declare that there is no conflict of interests regarding the publication of the paper.

Author Contribution

*The authors confirm contribution to the paper as follows: **study conception and design:** Ahmad Zaki, Ni Nyoman Kencanawati, Syarizal Fonna, Zainah Ibrahim; **data collection:** Ahmad Zaki, Sri Atmaja P. Rosyidi; **analysis and interpretation of results:** Ahmad Zaki, Hammad R. Khalid, M.A. Al-Osta; **draft manuscript preparation:** Ahmad Zaki, Sri Atmaja P. Rosyidi, Hammad R. Khalid. All authors reviewed the results and approved the final version of the manuscript.*

References

[1] Wilburn, D. R., & Goonan, T. G. (1998). Aggregates From Natural and Recycled Sources. US Geological Survey Circular, 1176, pp. 36.

[2] Shafigh, P., Jumaat, M. Z., & Mahmud, H. (2011). Oil palm shell as a lightweight aggregate for production high strength lightweight concrete. Construction and Building Materials, 25(4), 1848-1853.

[3] Shigetomi, Y., Ishimura, Y., & Yamamoto, Y. (2020) Trends in global dependency on the Indonesian palm oil and resultant environmental impacts. Scientific Reports, 10(1), 20624.

[4] Purba, J. H. V. (2019. Replanting policy of Indonesian palm oil plantation in strengthening the implementation of sustainable development goals. IOP Conference Series: Earth and Environmental Science, 012012.

[5] Abdullah, N., & Sulaiman, F. (2013). The oil palm wastes in Malaysia. In M. D. Matovic (Eds), *Biomass now-sustainable growth and use* (pp. 75-93). IntechOpen.

[6] Yap, S. P., Alengaram, U. J., Mo, K. H., & Jumaat, M. Z. (2017) High strength oil palm shell concrete beams reinforced with steel fibres. Materiales de Construcción, https://doi.org/10.3989/mc.2017.11616.

[7] Kristianto, K., Mungok, C. D., & Handalan, C. P. (2016). The effect of using palm oil shells as an additive on concrete quality, Thesis, Tanjungpura University.

[8] Merriza, S., Aulia, T. B., & Hasan, M. (2016). Analysis of shear capacity of high quality reinforced concrete variations of additives and aggregate substitution (palm shell). Jurnal Teknik Sipil, 6(1), 77-92.

[9] Lee, S. T., Handika, N., Tjahjono, E., & Arijoeni, E. (2019). Study on the effect of pre-treatment of oil palm shell (OPS) as coarse aggregate using hot water 50°C and room temperature water 28°C to lightweight concrete strength. MATEC Web of Conferences, 01023.

[10] Huda, M. N., Jumaat, M. Z., Islam, A. S., & Al-Kutti, W. A. (2018). Performance of high strength lightweight concrete using palm wastes. IIUM Engineering Journal, 19(2), 30-42.

[11] Danso, H., & Appiah-Agyei, F. (2021, June 16-18). A Study on Size Variation of Palm Kernel Shells as Replacement of Coarse Aggregate for Lightweight Concrete Production. 4th International Conference on Bio-based building Materials, Barcelona, Spain.

[12] Fani, A. M., Handika, N., Tjahjono, E., & Arijoeni, E. (2019). Flexural behaviour of reinforced lightweight concrete floor panel using hot water pre-treated oil palm shell as coarse aggregate. AIP Conference Proceedings, 040001.

[13] Aslam, M., Shafigh, P., & Jumaat, M. Z. (2017). High strength lightweight aggregate concrete using blended coarse lightweight aggregate origin from palm oil industry. Sains Malaysiana, 46(4), 667-675.

[14] Shafigh, P., Salleh, S., Ghafari, H., & Mahmud, H. (2018). Oil palm shell as an agricultural solid waste in artificial lightweight aggregate concrete. European Journal of Environmental and Civil Engineering, 22(2), 165-180.

[15] Tjahjono, E., A. M., Dodi, D. D., Purnamasari, E. P., Silaban, F.A., & Arijoeni, E. (2017). The study of oil palm shell (OPS) lightweight concrete using superplasticizer, silica fume, and fly ash. Materials Science Forum, pp. 65-73.

[16] Maghfouri, M., Shafigh, P., & Aslam, M. (2018). Optimum oil palm shell content as coarse aggregate in concrete based on mechanical and durability properties. Advances in Materials Science and Engineering, https://doi.org/10.1155/2018/4271497.

[17] Azunna, S. U. (2019). Compressive strength of concrete with palm kernel shell as a partial replacement for coarse aggregate. SN Applied Sciences, 1(4), 1-10.

[18] Khan, M., Guong W. L., Deepak T. J., & Nair, S. (2016). Use of oil palm shell as replacement of coarse aggregate for investigating properties of concrete. International Journal of Applied Engineering Research, 11(4), 2379-2383.

[19] Wibisono, C.A., Zaki, A., Saleh F., & Fauzi, A. (2023). The effect of partial replacement of aggregate on the flexural strength of corroded oil palm shell concrete, AIP Conference Proceedings, https://doi.org/10.1063/5.0117080.

[20] Rahayu, H., Zaki, A., Saleh, F., & Fauzi, A. (2023). The effect of different acceleration corrosion processes on flexural strength of oil palm shell concrete, AIP Conference Proceedings, https://doi.org/10.1063/5.0110423.

[21] Zaki, A., Kirana, I. R .A., Shodiq, M. I., Wibisono, C. A., & Saleh, F. (2023). The effect of curing on flexural strength of concrete with oil palm shells as a substitute for coarse aggregate, AIP Conference Proceedings, https://doi.org/10.1063/5.0154960.

[22] Siddika, A., Al Mamun, M. A., Alyousef, R., & Amran, Y. M. (2019). Strengthening of reinforced concrete beams by using fiber-reinforced polymer composites: A review. Journal of Building Engineering, https://doi.org/10.1016/j.jobe.2019.100798.

[23] Zaki, A., Yadi S., Khoirullianum, E., Suganda R., & Wibisono, C. A. (2024). Effect of partial replacement of aggregate with oil palm shell on compressive and flexural strength of fiber concrete. Multidisciplinary Science Journal, https://doi.org/10.31893/multiscience.2024102.

[24] Zaki, A., Fikri, M. A., Wibisono C. A., & Rosyidi, S. A. P. (2023). Evaluating pre-corrosion and post-corrosion of oil palm shell concrete with non-destructive testing. Key Engineering Materials, https://doi.org/10.4028/p-9qfaiq.

[25] Sangkham, S. (2020) Face mask and medical waste disposal during the novel COVID-19 pandemic in Asia, Case Studies in Chemical and Environmental Engineering, 2, 100052. https://doi.org/10.1016/j.cscee.2020.100052

[26] Kilmartin-Lynch S., Saberian, M., Li J., Roychand R., & Zhang, G. (2021). Preliminary evaluation of the feasibility of using polypropylene fibres from COVID-19 single-use face masks to improve the mechanical properties of concrete, Journal of Cleaner Production, 296, 126460. https://doi.org/10.1016/j.jclepro.2021.126460

[27] Abd El Aal, A., Abdullah G. M., Qadri, S. T., Abotalib, A. Z., & Othman, A. (2022). Advances on concrete strength properties after adding polypropylene fibers from health personal protective equipment (PPE) of COVID-19: Implication on waste management and sustainable environment, Physics and Chemistry of the Earth, Parts A/B/C, 128, 103260. https://doi.org/10.1016/j.pce.2022.103260

[28] Koniorczyk, M., Bednarska, D., Masek, A., & Cichosz, S. (2022) Performance of concrete containing recycled masks used for personal protection during coronavirus pandemic, Construction and Building Materials, 324, 126712. https://doi.org/10.1016/j.conbuildmat.2022.126712

[29] Zhang, Y., Li, N., Lv, G., & Chen, Z. (2019). Quantification of fatigue damage at dry–wet cycles of polymer fiber cement mortar. Materials Letters, 257, 126754. https://doi.org/10.1016/j.matlet.2019.126754

[30] Aswin, M., Iqlima, M., & Alfarizy, R. A. (2023). Consideration on use of the corn plant ash-based concrete related to the salt and acid attack: A review. Journal of Physics: Conference Series, 012039.

[31] Sukardjo, S., & Afriadi, R. (2015). Coastal zone space in Indonesia: Prelude to conflict?. International Journal of Development Research, 5(01), 2992-3012.

[32] Harahap, S., Puspitasari, S. D., & Muhaimin, A. A. (2023). Seawater-mixed concrete in Indonesia and anti-corrosive materials: A review. AIP Conference Proceedings, 2482(1), 050002. https://doi.org/10.1063/5.0110946.

[33] Wang, G., Wu, Q., Zhou, H., Peng, C., & Chen, W. (2021). Diffusion of chloride ion in coral aggregate seawater concrete under marine environment, Construction and Building Materials, 284, 122821

[34] Qu, F., Li, W., Dong, W., Tam, V. W. Y., & Yu, T. (2021). Durability deterioration of concrete under marine environment from material to structure: A critical review. Journal of Building Engineering, 35, 102074.

[35] Alomayri, T., Ali, B., Raza, S. S., Ahmed, H., & Hamad, M. (2023). Investigating the effects of polypropylene fibers on the mechanical strength, permeability, and erosion resistance of freshwater and seawater mixed concretes. Journal of Marine Science and Engineering, https://doi.org/10.3390/jmse11061224.

[36] Yuan Z., & Jia, Y. (2021). Mechanical properties and microstructure of glass fiber and polypropylene fiber reinforced concrete: An experimental study. Construction and Building Materials, 266, 121048.

[37] Abdulkareem, O., Alshahwany R., & Abdullah Mousa, A. (2022). Durability of polypropylene fiber reinforced concrete: Literatures review. Electronic Journal of Structural Engineering, https://doi.org/10.1155/2021/6652077.

[38] Rodrigues, R. Gaboreau, S. Gance, J. Ignatiadis I., & Betelu, S. (2021). Reinforced concrete structures: A review of corrosion mechanisms and advances in electrical methods for corrosion monitoring. Construction and Building Materials, 269, 121240.

[39] Tian, Y., Zhang G., Ye, H., Zeng, Q., Zhang, Z., Tian, Z., Jin, X., Jin, N., Chen, Z., & Wang, J. (2023). Corrosion of steel rebar in concrete induced by chloride ions under natural environments. Construction and Building Materials, 369, 130504.

[40] Yap, S. P., Alengaram U. J., & Jumaat, M. Z. (2013). Enhancement of mechanical properties in polypropylene and nylon–fibre reinforced oil palm shell concrete. Materials & Design, 49, 1034-1041.

[41] Yew, M. K., Mahmud, H. B., Ang B. C., & Yew M. C. (2015). Influence of different types of polypropylene fibre on the mechanical properties of high-strength oil palm shell lightweight concrete. Construction and Building Materials, 90, 36-43.

[42] Mo, K. H., Alengaram U. J., & Jumaat, M. Z. (2015). Utilization of ground granulated blast furnace slag as partial cement replacement in lightweight oil palm shell concrete. Materials and Structures, 48(8), 2545-2556.

[43] Yap, S. P., Alengaram U. J., & Jumaat, M. Z. (2016). The effect of aspect ratio and volume fraction on mechanical properties of steel fibre-reinforced oil palm shell concrete. Journal of Civil Engineering and Management, 22(2), 168-177.

[44] Prusty J. K., & Patro, S. K. (2015). Properties of fresh and hardened concrete using agro-waste as partial replacement of coarse aggregate – A review. Construction and Building Materials, 82, 101-113.

[45] SK SNI 2834-2000 (2000). The procedure for making a normal concrete mix plan. Badan Standar Nasional Indonesia.

[46] ASTM G1-03 (2004). Standard Practice for Preparing, Cleaning, and Evaluating Corrosion Test Specimens. American Society for Testing and Materials.

[47] ASTM G31-72 (2004). Standard practice for laboratory immersion corrosion testing of metals. American Society for Testing Materials.

[48] Zaki A., & Ibrahim, Z. (2021). Corrosion assessment of pre-corrosion concrete specimens using acoustic emission technique. Journal of Engineering and Technological Sciences, https://doi.org/10.5614/j.eng.technol.sci.2021.53.2.11.

[49] SNI ASTM C136: 2012 (2012). Test method for sieve analysis of fine aggregate and coarse aggregate. Badan Standar Nasional Indonesia.

[50] Shafigh, P. Jumaat M. Z., & Mahmud, H. (2010). Mix design and mechanical properties of oil palm shell lightweight aggregate concrete: A review. International Journal of the Physical Sciences, 5(14), 2127-2134.

[51] Orouji, M., Zahrai S. M., & Najaf, E. (2021). Effect of glass powder & polypropylene fibers on compressive and flexural strengths, toughness and ductility of concrete: an environmental approach. Structures, 33, 4616-4628. https://doi.org/10.1016/j.istruc.2021.07.048

[52] Naderpour, H. Ghasemi-Meydansar, F., & M. Haji (2022). Experimental study on the behavior of RC beams with artificially corroded bars. Structures, 43, 1932-1944. https://doi.org/10.1016/j.istruc.2022.07.005

[53] Shafigh, P. Jumaat, M. Z. Mahmud H. B., & Alengaram U. J. (2011). A new method of producing high strength oil palm shell lightweight concrete. Materials & Design, 32(10), 4839-4843. https://doi.org/10.1016/j.matdes.2011.06.015

[54] Hosen M. A., Shammas, M. I., Shill, S. K., Al-Deen, S., Jumaat M. Z., & Hashim, H. (2022). Ductility enhancement of sustainable fibrous-reinforced high-strength lightweight concrete. Polymers, 14(4), 727. https://doi.org/10.3390/polym14040727

[55] Cui, J., Qi, M., Zhang Z., Gao, S., Xu, N., Wang, X., Li, N., & Chen, G. (2023). Disposal and resource utilization of waste masks: a review. Environmental Science and Pollution Research, 30(8), 19683-19704. https://doi.org/10.1007/s11356-023-25353-6

[56] Kareem, M., Raheem, A., Oriola, K., & Abdulwahab, R. (2022). A review on application of oil palm shell as aggregate in concrete-Towards realising a pollution-free environment and sustainable concrete. Environmental Challenges, 8, 100531. https://doi.org/10.1016/j.envc.2022.100531

[57] Masoule, M. S. T., Bahrami, N., Karimzadeh, M., Mohasanati, B., Shoaei, P., Ameri F., & Ozbakkaloglu T. (2022) Lightweight geopolymer concrete: A critical review on the feasibility, mixture design, durability properties, and microstructure. Ceramics International, 48(8), 10347-10371. https://doi.org/10.1016/j.ceramint.2022.01.298

[58] Robles, K. P. V., Yee, J. J., & Kee, S. H. (2022). Electrical resistivity measurements for nondestructive evaluation of chloride-induced deterioration of reinforced concrete - A review. Materials, 15(8), 2725. https://doi.org/10.3390/ma15082725

[59] Zaki, A., Rahayu, H., Nugraha D. A., Rosyidi, S. A. P., Kencanawati N. N., & Fonna, S. (2024). Resistivity method evaluation of corroded OPS-concrete. E3S Web Conference, 476, 01037. https://doi.org/10.1051/e3sconf/202447601037

[60] Golewski, G. L. (2023). The phenomenon of cracking in cement concretes and reinforced concrete structures: The mechanism of cracks formation, causes of their initiation, types and places of occurrence, and methods of detection - A review, Buildings, 13(3), 765. https://doi.org/10.3390/buildings13030765

[61] Farhangdoust, S., & Mehrabi, A. (2019). Health monitoring of closure joints in accelerated bridge construction: A review of non-destructive testing application. Journal of Advanced Concrete Technology, 17(7), 381-404. https://doi.org/10.3151/jact.17.381.